analytical chemistry

pubs.acs.org/ac

Technical Note

Investigation of Charged Small Molecule−Aptamer Interactions with Surface Plasmon Resonance

Clarice E. Froehlich, Jiayi He, and Christy L. Haynes*

Cite This: *Anal. Chem.* 2023, 95, 2639−2644

Read Online

ACCESS | Metrics & More | Article Recommendations | Supporting Information

ABSTRACT: Investigating the interactions between small, charged molecules and aptamers using surface plasmon resonance (SPR) is limited by the inherent low response of small molecules and difficulties with nonspecific electrostatic interactions between the aptamer, analyte, and sensor surface. However, aptamers are increasingly being used in sensors for small molecule detection in critical areas like healthcare and environmental safety. The ability to probe these interactions through simple, direct SPR assays would be greatly beneficial and allow for the development of improved sensors without the need for complicated signal enhancement. However, these assays are nearly nonexistent in the current literature and are instead surpassed by sandwich or competitive binding techniques, which require additional sample preparation and reagents. In this work, we develop a method to characterize the interaction between the charged small molecule serotonin (176 Da) and an aptamer with SPR using streptavidin−biotin capture and a high-ionic-strength buffer. Additionally, other methods, such as serotonin immobilization and thiol-coupling of the aptamer, were investigated for comparison. These techniques give insight into working with small molecules and allow for quickly adapting a binding affinity assay into a direct SPR sensor.

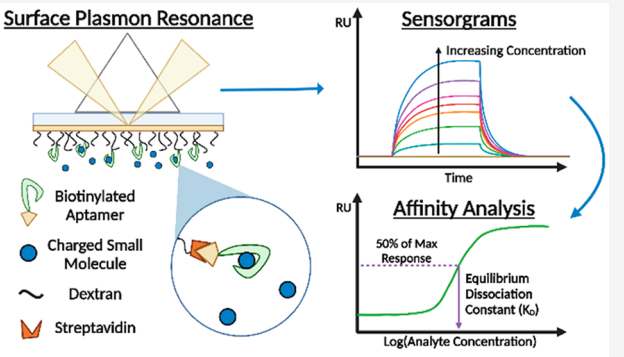

INTRODUCTION

Small, charged molecules like serotonin are vital targets for detection given their importance in clinical diagnostics,[1−3] drug discovery and disease treatment,[4−6] food safety,[7,8] environmental protection,[9,10] and other areas.[11,12] However, these analytes are difficult to detect and quantify at their often very low relevant concentrations due to their small size, generally yielding low signal intensity in optical or colorimetric sensors.[13] While antibodies are the traditional affinity and capture agents used for various sensors like enzyme-linked immunosorbent assays (ELISA) or surface plasmon resonance (SPR), there are not many natural antibodies for small molecules since they are typically not immunogenic.[14] However, newer types of affinity agents have been developed which are much more easily obtained for small molecules, such as aptamers, which are single-stranded oligonucleotides selected for a specific target using systematic evolution of ligands by exponential enrichment (SELEX).[15,16] Aptamers have been increasingly used as affinity agents to capture analytes in sensors due to their many advantages over antibodies, including stability, tunability of affinity and selectivity, low cost, in vitro synthesis, reproducibility, and ability to be easily chemically modified.[17,18] Aptamer-based sensors have been used for many clinically and environmentally relevant small, charged molecules such as neurotransmitters (e.g., serotonin,[19] dopamine,[20] and histamine[21]), pesticides (e.g., glyphosate[16] and imidacloprid[22]), toxins (e.g., ochratoxin A),[23] and drugs (e.g., tenofovir).[24]

To develop and improve sensors, it is important to effectively characterize the interactions between affinity agents and their targets of interest using methods such as isothermal titration calorimetry (ITC), fluorescence quenching, or SPR.[25−27] Of these, SPR provides advantages of being able to analyze both affinity and kinetics, requiring no labels, and being able to use the characterization platform directly as a quantitative sensor.[27,28] The underlying principle of SPR is that the excitation of surface plasmons is dependent on the refractive index of the media surrounding the gold sensor surface where ligands are attached, which allows for detection of binding events through changes in absorption and reflection of light by the metal. While examples of traditional antibody−antigen interactions are numerous in the SPR literature,[29−35] those involving charged small molecule−aptamer interactions are highly uncommon,[36] and examples using direct methods tend to only involve detection and not affinity character-

Received: September 22, 2022
Accepted: January 11, 2023
Published: January 27, 2023

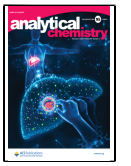

https://doi.org/10.1021/acs.analchem.2c04192
Anal. Chem. 2023, 95, 2639−2644

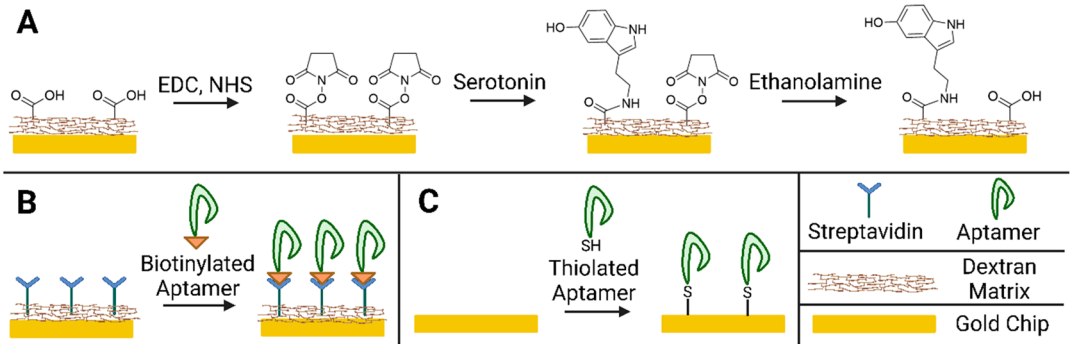

Figure 1. Procedures for immobilization on the SPR chip surface. (A) Amine coupling of serotonin to carboxylic acid groups on the dextran layer of a Biacore CM5 sensor chip. EDC and NHS are 1-ethyl-3-(3-(dimethylamino)propyl)carbodiimide and *N*-hydroxysuccinimide, respectively. (B) Capture of biotinylated aptamer on the Biacore SA sensor chip which is coated with a streptavidin-functionalized dextran layer. (C) Thiol-coupling of aptamer to the bare gold Biacore Au sensor chip. Created with BioRender.com.

ization.[37,38] This could likely be due to analytical challenges associated with both aptamers and small molecules in these types of sensors. For example, the low molecular weight of small molecules, especially those under 300 Da, generates an inherently weak SPR signal, making their interactions difficult to probe.[39−41] This usually means that more complicated methods, such as competition or sandwich assays,[42−45] or signal enhancement methods, such as with plasmonic nanoparticles,[42,44,46,47] must be used. Additionally, aptamers can be more difficult to immobilize on SPR chips than antibodies, given their high density of negative charge, which is repelled from the negatively charged carboxymethylated dextran that typically coats SPR chip surfaces to allow for a greater surface area available for binding. For these reasons, alternative methods to standard amine coupling are required for aptamer immobilization, such as streptavidin−biotin coupling[48] or cDNA capture.[49] Targeting charged molecules adds an additional layer of complication to SPR assays, since nonspecific electrostatic interactions can cause attraction or repulsion of the target from the chip surface and from the aptamer itself, making sensitive and accurate measurements difficult. Herein, we address these numerous challenges and develop a simple, direct SPR assay to characterize the affinity of a charged small molecule−aptamer interaction, using serotonin (176 Da) and a previously selected aptamer[50] as a model system. The use of streptavidin−biotin capture for the aptamer as well as a high-ionic-strength running buffer were successful; however, other methods like immobilization of the small molecule and thiol-coupling of the aptamer to bare gold were also explored, and their pitfalls are discussed. These results are applicable to the investigation of many aptamer−small molecule systems, and allow for streamlined protocols and analyses for interaction characterizations which can also be quickly adapted into SPR sensors.

EXPERIMENTAL SECTION

Materials and Chemicals. Three aptamers were purchased as DNA oligomers with different functionalization, all with the sequence 5′-CTC-TCG-GGA-CGA-CTG-GTA-GGC-AGA-TAG-GGG-AAG-CTG-ATT-CGA-TGC-GTG-GGT-CGT-CCC-3′. The unmodified, thiolated, and biotinylated aptamers were purchased with no modification, 5′ thiol C6 and 5′ biotin, respectively, along with TE buffer (10 mM Tris pH 8.0, 0.1 mM EDTA) from IDT (Integrated DNA Technologies, Coralville, IA). An aptamer with random sequence 5′-biotin-TTA-CTG-CGG-ACC-ATG-TCG-TCC-TCA-TAG-TTT-GGG-CAT-GTT-TCC-GTT-GTA-GGA-GTG-AAG-3′ was also purchased from IDT. The aptamers were purified by standard desalting and dried. PBS buffer was purchased from Fisher Bioreagents (Hampton, NH). Tris[2-carboxyethyl] phosphine (TCEP) was obtained from Thermo Fisher Scientific (Waltham, MA). Biacore Series S CM5, SA, and Au sensor chips; HBS-EP and PBS-P+ buffers; 1-ethyl-3-(3-(dimethylamino)propyl)carbodiimide (EDC); *N*-hydroxysuccinimide (NHS); and ethanolamine hydrochloride were purchased from Cytiva Life Sciences (Marlborough, MA). Serotonin hydrochloride was obtained from Alfa Aesar (Ward Hill, MA).

Aptamer Immobilization via Biotin−Streptavidin Capture. SPR experiments were conducted on a Biacore S200 instrument (Cytiva Life Sciences) set at 25 °C. Aptamer immobilization via capture was performed using a Series S SA sensor chip with 0.22 μm filtered PBS-P+ running buffer (pH 7.4) by injecting 75.3 μM biotinylated aptamer in PBS at 10 μL/min for 7 min followed by a 3 min PBS-P+ buffer injection at 10 μL/min.

High-Ionic-Strength Multicycle SPR Assay. Biotinylated aptamer was immobilized on one flow cell of a Series S SA sensor chip, using PBS-P+ with 1 M NaCl as the running buffer and as the buffer for sample solutions. Assay injections were made over the immobilized flow cell and a blank reference flow cell. Sample cycle settings were set as high performance with sample injections of 120 s contact and 600 s dissociation at 20 μL/min with no regeneration injection. For the assay using the random-sequence aptamer, a dissociation time of 180 s was used, with all other parameters remaining the same. A startup cycle was run with sample cycle settings and running buffer as the sample. Three replicates were run for each serotonin concentration (0, 0.1 nM, 1 nM, 10 nM, 100 nM, 500 nM, 1 μM, 10 μM, 50 μM, and 100 μM) using sample cycle settings.

Data Analysis. Affinity was determined by fitting serotonin concentration versus steady-state binding response to a 1:1 equilibrium binding equation (eq 1) involving the dissociation equilibrium constant K_d, the maximum binding response occurring at saturation R_{max}, and the offset value, which is the binding response at zero concentration.

$$R_{eq} = \frac{R_{max}[S]}{K_d + [S]} + (\text{offset}) \quad (1)$$

https://doi.org/10.1021/acs.analchem.2c04192
Anal. Chem. 2023, 95, 2639−2644

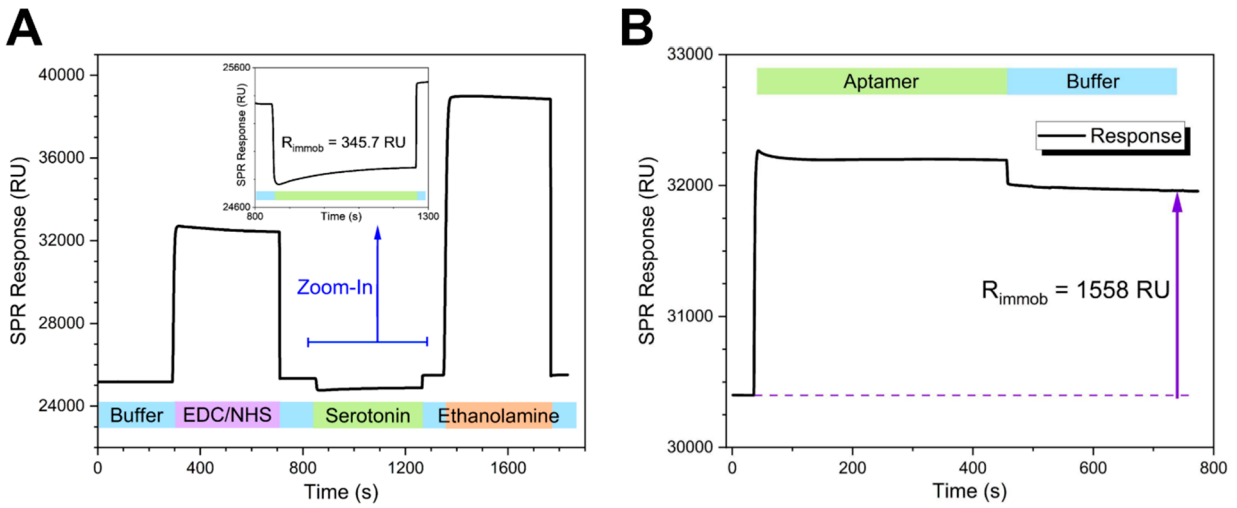

Figure 2. (A) Sensorgram for immobilization of serotonin on an SPR sensor chip surface. The response shown is for the active flow cell during immobilization. Purple, green, blue, and orange boxes represent the duration of buffer, EDC/NHS, serotonin, and ethanolamine flow, respectively. The inset figure zooms in on the region where serotonin injection occurs, with the immobilized amount of serotonin given. (B) Immobilization of biotinylated aptamer on the SPR sensor chip surface. The green and blue boxes indicate the duration of the aptamer injection and the PBS-P+ buffer wash, respectively. A purple arrow indicates the overall response corresponding to the immobilized aptamer.

RESULTS AND DISCUSSION

Since serotonin has a low molecular weight (176 Da) which is nearly at the practical lower limit for the SPR instrument (specified as 100 Da),[39] immobilizing serotonin on the SPR chip surface as the ligand and using the aptamer (17.7 kDa) as the binding analyte theoretically allows for greater measurement sensitivity since responses would be of a higher magnitude. As shown in eq 2, the theoretical maximum response ($R_{max,t}$) from an analyte is when all binding sites are saturated, and it gives a measure of the expected response. $R_{max,t}$ can be calculated by correcting the immobilized amount of ligand (R_{immob}) with the ratio of the molecular weights of the analyte and ligand ($M_{analyte}$ and M_{ligand}). Thus, due to the difference in their molecular weights, serotonin as an analyte would have a response 100 times lower than the same molar concentration of aptamer.

$$R_{max,t} = \frac{M_{analyte}}{M_{ligand}} R_{immob} \quad (2)$$

Serotonin was immobilized via amine coupling through EDC/NHS chemistry to carboxy groups on the chip's dextran layer, as illustrated in Figure 1A.[51,52] As shown in Figure 2A, from the start to finish of immobilization, which goes from before the EDC/NHS activation to after deactivation of remaining active groups using ethanolamine, the SPR response increased by 345.7 RU. This corresponds to the amount of serotonin immobilized, and it is relatively high compared with theoretical values for serotonin, since it is a small molecule.

To test the binding response, 256 nM unmodified serotonin aptamer was injected over the chip surface (Figure S1). The measured response increased quickly to a steady state value of 3.7 to 4.3 RU during each of the injections, and quickly decreased back to the baseline value of 1 ± 2 RU once the aptamer injection finished. This response is very low in comparison to what would be expected from eq 2 for such a large analyte (17.7 kDa), as this should be at least on the order of tens of thousands of RU. These results suggest that the aptamer was not binding to the immobilized serotonin. The response that did occur is likely a nonspecific effect from aptamer flowing over the chip surface and not binding. Since it is known from the literature that this aptamer has an affinity for serotonin with an in-solution K_d of approximately 30 nM,[50] this leads to a few possible conclusions: the aptamer may not be able to bind due to steric constraints from serotonin being bonded to the chip surface; negatively charged carboxy groups on the chip surface may be electrostatically repelling the negatively charged aptamer; or the amine group on the serotonin molecules may play a vital role in its binding interaction with the aptamer. It is likely for the vast majority of small molecules that coupling to the chip surface would affect or prevent the binding interaction due to the low number of functional groups on each molecule, and the necessary functional groups for coupling to dextran would need to be present in the first place. Thus, despite the low-signal issues that come with using serotonin as the analyte, immobilization of the aptamer could resolve some of these issues and create a platform allowing for the detection of serotonin as well as the determination of binding characteristics. Furthermore, immobilizing the aptamer is advantageous as it provides similar conditions in which the interaction would occur on many sensing platforms, like field effect transistors, where the aptamer is surface-bound, so it is more relevant to developing these other sensors as well.

For immobilizing negatively charged nucleic acids in SPR, electrostatic preconcentration at the chip surface is generally not feasible since the dextran matrix (pI ~5) also has a negative charge in the running buffer (pH 7.4), and the pH cannot be tuned so that they attract each other through opposite charges. In order to avoid electrostatic repulsion of the aptamer from the chip surface, the aptamer can be immobilized on a bare gold surface without dextran as shown in Figure 1C. However, as can be seen in Figure S2, immobilization of thiolated aptamer directly on the gold surface of a sensor chip yields an immobilized signal of 422.6 RU, which gives a very low $R_{max,t}$ of 4.2 RU. This does not allow for much sensitivity due to limitations in the measurement of small responses by the instrument. Additionally, a

https://doi.org/10.1021/acs.analchem.2c04192
Anal. Chem. 2023, 95, 2639−2644

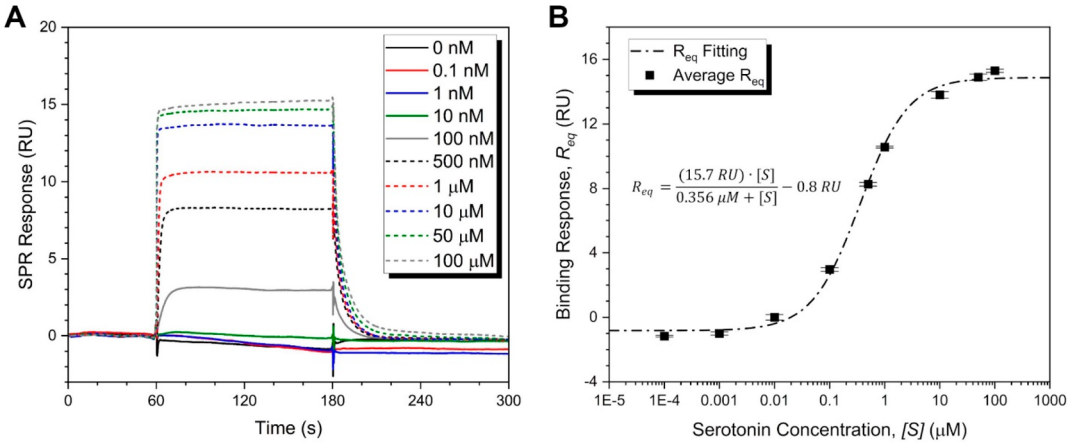

Figure 3. (A) Sensorgrams for multicycle assay using PBS-P+ buffer with high ionic strength (1 M NaCl) and serotonin concentrations from 0.1 nM to 100 μM. Samples were injected during the 60−180 s time period, with PBS-P+ with 1 M NaCl running buffer being injected at other times. The response given is that of the active flow cell minus the reference flow cell. (B) Logarithmic scale serotonin concentration, $[S]$, versus average equilibrium binding response, R_{eq}, for three replicates of a multicycle SPR assay using high-ionic-strength PBS-P+ buffer. Error bars represent standard deviation. The dashed line represents the fitting of the experimental results to a steady-state binding equation as given to the left of the curve.

high-ionic-strength buffer was used for the aptamer in this immobilization to screen charges and reduce repulsion between negatively charged aptamers, but the amount of aptamer immobilized remained low. The predominant issue with this method is that immobilizing a thiolated aptamer directly on the 2D gold chip surface limits movement and provides less area for aptamers to attach, as compared to a 3D dextran-coated surface which has a much larger number of available sites for aptamer attachment. Thus, the streptavidin−biotin capture technique was chosen to immobilize the aptamer; it is a common technique for immobilizing nucleic acids[53−55] since it does not require electrostatic preconcentration of the ligand at the chip surface, allows for less constrained movement of the aptamer to avoid steric hindrances during binding, and allows a higher density of immobilized aptamer due to the 3D dextran matrix which the streptavidin is attached to. While there is a commercial chip (Biacore CM7) available for working with small molecules, it was not used here as it has a higher degree of carboxylation which would increase repulsion of the aptamer from the chip surface due to their like charges.

Here, the streptavidin−biotin immobilization method uses a gold sensor chip coated with carboxymethylated dextran that has been functionalized with streptavidin. Biotin is covalently linked to the end of the aptamer so that, in a single-step immobilization, the biotinylated aptamer is flowed over the surface and captured by streptavidin, as illustrated in Figure 1B. Additionally, biotin has a very high affinity for streptavidin (K_d = 1 fM),[56] so this capture technique allows for the aptamer to be strongly bound to the surface such that it will not be removed by flowing buffer. The sensorgram for an aptamer immobilization via streptavidin capture is shown in Figure 2B. The overall increase in response of 1558 RU shows that aptamer was captured and immobilized on the sensor chip surface. Using eq 2, this yields a theoretical R_{max} of about 15.6 RU.

Due to the decreasing baseline observed in the single-cycle assay (Figure S3), further studies used a multicycle assay format, where a new baseline response level is taken after every sample injection rather than after all injections in a series, have been completed, as in single-cycle assays. This is especially important for small molecules because the response values are low, so even small changes in the baseline can have significant effects on measured binding response. Since the literature K_d value of 30 nM was found in solution using fluorescence measurements,[50] the K_d found using SPR may be higher since the interaction is surface-bound. As such, a higher range of concentrations (2 μM to 1000 μM) was tested in the multicycle assay as shown in Figure S4. In this assay, responses increased with concentration but clearly did not level off near the theoretical R_{max}. This leads to the conclusion that nonspecific binding is occurring on the sensor surface, causing higher responses than should be possible if the only interactions are specific 1:1 binding to the aptamer. The source of these nonspecific interactions is likely the electrostatic attraction of serotonin to the chip surface. Serotonin has a pK_a of 10,[57] so in the buffer of pH 7.4, it is in a protonated, positively charged state. Thus, serotonin is attracted to the negatively charged aptamer and the negatively charged carboxyl groups on the dextran layer (pI = 5), with streptavidin not playing a role since it is uncharged at this pH.[58]

To suppress the effect of these electrostatic interactions, a high concentration of salt (1 M NaCl) was added to the running buffer and analyte buffer to minimize the impact of electrostatics on SPR response compared to that from specific serotonin−aptamer binding interactions.[61] This technique of using a higher-ionic-strength buffer is also applicable to other small molecules with positive or negative charges at the buffer pH, such as glyphosate[59] or dopamine,[60] as it helps prevent attraction or repulsion of analytes from the chip surface due to the charge of the dextran layer.

For the high-ionic-strength-facilitated experiments, PBS-P+ with 1 M NaCl was used, and the immobilization of the aptamer followed the previously established protocol. As can be seen in Figure S5, the immobilized amount of aptamer was 1813.2 RU. The decrease in response during the aptamer injection occurred because the aptamer buffer did not contain the added salt of the running buffer, so it had a lower refractive index. However, since the response after the buffer wash was higher than prior to aptamer injection, this indicates that

https://doi.org/10.1021/acs.analchem.2c04192
Anal. Chem. 2023, 95, 2639−2644

aptamer was immobilized. This high-ionic-strength buffer technique was then used to reduce electrostatic interactions in a multicycle assay with three replicates and a wide range of serotonin concentrations from 0.1 nM to 100 μM; the resulting sensorgrams are shown in Figure 3A. Association and dissociation curvature is observed for concentrations above 1 nM, and the blank response was negligible, which suggests binding was occurring between serotonin and the aptamer. It is also apparent that the high ionic strength effectively screened charges at the tested concentrations of serotonin, since the binding responses plateaued just below the theoretical R_{max} of 18 RU, as would be expected.

The steady-state binding responses were fitted to the affinity model in eq 1, as shown in Figure 3B, which yielded a K_d of 360 nM. There is some deviation from the fit at the higher concentrations, though this is potentially due to charge screening by the high ionic strength being less effective at higher serotonin concentrations. Further, each replicate was fitted individually to eq 1, finding K_d values that were in agreement within 10 nM. The closeness of the fit was measured by calculating χ^2 values as the average of the squared residuals from the fitting. A χ^2 value of less than 10% of R_{max} indicates a good fit, a criterion that was met for each replicate individually and for the combined replicates, as shown in Table S1. Thus, the K_d for the aptamer−serotonin interaction in a surface-bound state was found to be 360 nM. This is an order of magnitude higher than the literature value of 30 nM,[50] though this is potentially due to differences between the conditions of the interaction. It would be expected that electrostatics typically promote the interaction due to the opposite charges of serotonin and the aptamer at the buffer pH, but this effect was suppressed here to reduce interactions with the chip surface.

A control experiment was performed using an aptamer with a random sequence, not specific to serotonin, replicating the other conditions of the high-ionic strength assay. As can be found in Figure S6, this showed low response values in comparison to those found when using the serotonin aptamer, and the binding responses increased up to approximately 3 RU only at the very high serotonin concentrations (50 and 100 μM) where charge screening of the high-ionic-strength buffer is less effective. As such, this control experiment helps to exemplify how the assay conditions were optimized for analysis of small, charged molecule interactions with aptamers.

CONCLUSIONS

Overall, we developed a method for investigating interactions between aptamers and very small, charged molecules that is applicable to a wide range of systems and has the potential to aid in the design of sensors for many small analytes such as neurotransmitters, pesticides, and mycotoxins. This method uses commercially available SPR sensor chips and easy immobilization procedures to allow for simple assays. It was concluded that streptavidin−biotin coupling of the aptamer is the best immobilization method for these systems, as immobilizing small molecules directly is likely to prevent their ability to bind. Moreover, aptamers are negatively charged and cannot be preconcentrated at the chip surface through the use of a low-pH immobilization buffer, and thiol-coupling to a bare gold sensor chip does not provide enough area to immobilize the large amount of aptamer needed for a sufficient serotonin binding response. Additionally, the use of a high-ionic-strength buffer was shown to reduce nonspecific interactions with the chip surface, though it can cause an overestimation of the K_d, possibly by up to an order of magnitude.

ASSOCIATED CONTENT

Supporting Information

The Supporting Information is available free of charge at https://pubs.acs.org/doi/10.1021/acs.analchem.2c04192.

Additional methods for aptamer preparation, serotonin immobilization, aptamer thiol-coupling, single cycle assays, low ionic strength assays, and extended data analysis; and additional figures and tables including aptamer injection over immobilized serotonin, aptamer thiol-coupling, the single cycle SPR assay, the low ionic strength SPR assay, high-ionic-strength aptamer immobilization, and fitting parameters for the affinity analysis (PDF)

AUTHOR INFORMATION

Corresponding Author

Christy L. Haynes − *Department of Chemistry, University of Minnesota, Minneapolis, Minnesota 55455, United States;* orcid.org/0000-0002-5420-5867; Email: chaynes@umn.edu

Authors

Clarice E. Froehlich − *Department of Chemistry and Department of Chemical Engineering and Materials Science, University of Minnesota, Minneapolis, Minnesota 55455, United States;* orcid.org/0000-0001-8862-785X

Jiayi He − *Department of Chemistry, University of Minnesota, Minneapolis, Minnesota 55455, United States*

Complete contact information is available at: https://pubs.acs.org/10.1021/acs.analchem.2c04192

Notes

The authors declare no competing financial interest.

ACKNOWLEDGMENTS

The authors would like to thank Kaitlyn Gruber and Casey Wouters for helpful discussions and assistance with running assays, and Casey Wouters and Beza Tuga for review of the manuscript, as well as Dr. Kevin Dorfman, Dr. C. Daniel Frisbie, and Demetra Adrahtas for support of the project. The S200 SPR instrument is supported with S10 Shared Instrument Grant 1S10OD021539-01 funded by the Office of Research Infrastructure Programs (ORIP)/NIH. Financial support for this work was provided primarily by the National Science Foundation through the University of Minnesota MRSEC under Award Number DMR-2011401.

REFERENCES

(1) Jungwirth, N.; Haeberle, L.; Schrott, K. M.; Wullich, B.; Krause, F. S. *World J. Urol* **2008**, *26* (5), 499−504.

(2) Hara, K.; Hirowatari, Y.; Yoshika, M.; Komiyama, Y.; Tsuka, Y.; Takahashi, H. *Journal of Laboratory and Clinical Medicine* **2004**, *144* (1), 31−37.

(3) Fröbe, A.; Čičin-Šain, L.; Jones, G.; Soldič, Ž.; Lukač, J.; Bolanča, A.; Kusič, Z. *Anticancer Res.* **2014**, *34* (3), 1167−1169.

(4) Shamsi, A.; DasGupta, D.; Alhumaydhi, F. A.; Khan, M. S.; Alsagaby, S. A.; al Abdulmonem, W.; Hassan, Md. I.; Yadav, D. K. *RSC Med. Chem.* **2022**, *13* (6), 737−745.

(5) Zhu, B.; Yang, J.; Van, R.; Yang, F.; Yu, Y.; Yu, A.; Ran, K.; Yin, K.; Liang, Y.; Shen, X.; Yin, W.; Choi, S. H.; Lu, Y.; Wang, C.; Shao, Y.; Shi, L.; Tanzi, R. E.; Zhang, C.; Cheng, Y.; Zhang, Z.; Ran, C. *Chem. Sci.* **2022**, *13* (27), 8104−8116.
(6) Scott, D. E.; Bayly, A. R.; Abell, C.; Skidmore, J. *Nat. Rev. Drug Discov* **2016**, *15* (8), 533−550.
(7) Wei, W.; Liu, C.; Ke, P.; Chen, X.; Zhou, T.; Xu, J.; Zhou, Y. *Food Chem. Toxicol.* **2021**, *151*, No. 112128.
(8) Chen, X.; Wu, H.; Tang, X.; Zhang, Z.; Li, P.Recent Advances in Electrochemical Sensors for Mycotoxin Detection in Food. *Electroanalysis***2021**, in press. DOI: 10.1002/elan.202100223.
(9) Lu, F.; Astruc, D. *Coord. Chem. Rev.* **2020**, *408*, No. 213180.
(10) Megharaj, M.; Ramakrishnan, B.; Venkateswarlu, K.; Sethunathan, N.; Naidu, R. *Environ. Int.* **2011**, *37* (8), 1362−1375.
(11) Fang, Z.; Weisenberger, M. C.; Meier, M. S. *ACS Appl. Bio Mater.* **2020**, *3* (2), 881−890.
(12) Donia, M. S.; Fischbach, M. A. *Science (1979)* **2015**, *349*, 6246.
(13) Wang, X.; Cohen, L.; Wang, J.; Walt, D. R. *J. Am. Chem. Soc.* **2018**, *140* (51), 18132−18139.
(14) Clementi, M. E.; Marini, S.; Condò, S. G.; Giardina, B. *Ann. Ist Super Sanita* **1991**, *27* (1), 139−143.
(15) de-los-Santos-Álvarez, N.; Lobo-Castañón, M. J.; Miranda-Ordieres, A. J.; Tuñón-Blanco, P. *TrAC Trends in Analytical Chemistry* **2008**, *27* (5), 437−446.
(16) Chergui, S.; Rhili, K.; Abrego-Martinez, J. C.; Jiménez, G. C.; Siaj, M. *ACS Agricultural Science & Technology* **2021**, *1* (6), 655−663.
(17) Cho, E. J.; Lee, J.-W.; Ellington, A. D. *Annual Review of Analytical Chemistry* **2009**, *2* (1), 241−264.
(18) Shaban, S. M.; Kim, D.-H. *Sensors* **2021**, *21* (3), 979.
(19) Nakatsuka, N.; Faillétaz, A.; Eggemann, D.; Forró, C.; Vörös, J.; Momotenko, D. *Anal. Chem.* **2021**, *93* (8), 4033−4041.
(20) Liu, X.; He, F.; Zhang, F.; Zhang, Z.; Huang, Z.; Liu, J. *Anal. Chem.* **2020**, *92* (13), 9370−9378.
(21) Mairal Lerga, T.; Jauset-Rubio, M.; Skouridou, V.; Bashammakh, A. S.; El-Shahawi, M. S.; Alyoubi, A. O.; O'Sullivan, C. K. *Anal. Chem.* **2019**, *91* (11), 7104−7111.
(22) Bor, G.; Man, E.; Ugurlu, O.; Ceylan, A. E.; Balaban, S.; Durmus, C.; Pinar Gumus, Z.; Evran, S.; Timur, S. *Electroanalysis* **2020**, *32* (9), 1922−1929.
(23) Cruz-Aguado, J. A.; Penner, G. *J. Agric. Food Chem.* **2008**, *56* (22), 10456−10461.
(24) Aliakbarinodehi, N.; Jolly, P.; Bhalla, N.; Miodek, A.; de Micheli, G.; Estrela, P.; Carrara, S. *Scientific Reports 2017 7:1* **2017**, *7* (1), 1−10.
(25) Freire, E.; Mayorga, O. L.; Straume, M. *Anal. Chem.* **1990**, *62* (18), 950A−959A.
(26) van de Weert, M.; Stella, L. *J. Mol. Struct.* **2011**, *998* (1−3), 144−150.
(27) Pattnaik, P. *Applied Biochemistry and Biotechnology 2005 126:2* **2005**, *126* (2), 79−92.
(28) Jönsson, U.; Fagerstam, L.; Ivarsson, B.; Johnsson, B.; Karlsson, R.; Lundh, K.; Lofas, S.; Persson, B.; Roos, H.; Ronnberg, I.; Sjolander, S.; Stenberg, E.; Stahlberg, R.; Urbaniczky, C.; Ostlin, H.; Malmqvist, M. *Biotechniques* **1991**, *11* (5), 620−627.
(29) Heinrich, L.; Tissot, N.; Hartmann, D. J.; Cohen, R. *J. Immunol Methods* **2010**, *352* (1−2), 13−22.
(30) Gupta, G.; Singh, P. K.; Boopathi, M.; Kamboj, D. v.; Singh, B.; Vijayaraghavan, R. *Thin Solid Films* **2010**, *519* (3), 1171−1177.
(31) Kikuchi, Y.; Uno, S.; Nanami, M.; Yoshimura, Y.; Iida, S. I.; Fukushima, N.; Tsuchiya, M. *J. Biosci Bioeng* **2005**, *100* (3), 311−317.
(32) Sikarwar, B.; Sharma, P. K.; Srivastava, A.; Agarwal, G. S.; Boopathi, M.; Singh, B.; Jaiswal, Y. K. *Biosens Bioelectron* **2014**, *60*, 201−209.
(33) Beeg, M.; Nobili, A.; Orsini, B.; Rogai, F.; Gilardi, D.; Fiorino, G.; Danese, S.; Salmona, M.; Garattini, S.; Gobbi, M. *Scientific Reports 2019 9:1* **2019**, *9* (1), 1−9.
(34) Real-Fernández, F.; Cimaz, R.; Rossi, G.; Simonini, G.; Giani, T.; Pagnini, I.; Papini, A. M.; Rovero, P. *Anal Bioanal Chem.* **2015**, *407* (24), 7477−7485.
(35) Medina, M. B. *J. Agric. Food Chem.* **1997**, *45* (2), 389−394.
(36) McKeague, M.; De Girolamo, A.; Valenzano, S.; Pascale, M.; Ruscito, A.; Velu, R.; Frost, N. R.; Hill, K.; Smith, M.; McConnell, E. M.; DeRosa, M. C. *Anal. Chem.* **2015**, *87* (17), 8608−8612.
(37) Sun, L.; Wu, L.; Zhao, Q. *Microchimica Acta* **2017**, *184* (8), 2605−2610.
(38) Zhu, Z.; Feng, M.; Zuo, L.; Zhu, Z.; Wang, F.; Chen, L.; Li, J.; Shan, G.; Luo, S. Z. *Biosens Bioelectron* **2015**, *65*, 320−326.
(39) *Biacore Assay Handbook*, Edition AA; General Electric Healthcare Bio-Sciences AB: Uppsala, Sweden, 2012.
(40) Karlsson, R.; Ståhlberg, R. *Anal. Biochem.* **1995**, *228* (2), 274−280.
(41) Yakes, B. J.; Kanyuck, K. M.; DeGrasse, S. L. *Anal. Chem.* **2014**, *86* (18), 9251−9255.
(42) Li, Y.; Sun, L.; Yu, H.; Zhao, Q. *ACS Food Science & Technology* **2022**, *2* (5), 936−940.
(43) Wang, J.; Zhou, H. S. *Anal. Chem.* **2008**, *80* (18), 7174−7178.
(44) Kim, S.; Lee, H. J. *Anal. Chem.* **2017**, *89* (12), 6624−6630.
(45) Moon, J.; Byun, J.; Kim, H.; Lim, E.-K.; Jeong, J.; Jung, J.; Kang, T. *Sensors* **2018**, *18* (2), 598.
(46) Matsui, J.; Akamatsu, K.; Hara, N.; Miyoshi, D.; Nawafune, H.; Tamaki, K.; Sugimoto, N. *Anal. Chem.* **2005**, *77* (13), 4282−4285.
(47) Tabasi, O.; Falamaki, C. *Analytical Methods* **2018**, *10* (32), 3906−3925.
(48) Hendrix, M.; Priestley, E. S.; Joyce, G. F.; Wong, C.-H. *J. Am. Chem. Soc.* **1997**, *119* (16), 3641−3648.
(49) L. Chang, A.; McKeague, M.; C. Liang, J.; D. Smolke, C. *Anal. Chem.* **2014**, *86* (7), 3273−3278.
(50) Nakatsuka, N.; Yang, K.-A.; Abendroth, J. M.; Cheung, K. M.; Xu, X.; Yang, H.; Zhao, C.; Zhu, B.; Rim, Y. S.; Yang, Y.; Weiss, P. S.; Stojanović, M. N.; Andrews, A. M. *Science (1979)* **2018**, *362* (6412), 319−324.
(51) Fischer, M. J. E.Amine Coupling Through EDC/NHS: A Practical Approach. In *Methods in Molecular Biology: Surface Plasmon Resonance*; Humana Press, 2010; Vol. *627*, pp 55−73. DOI: 10.1007/978-1-60761-670-2_3.
(52) Wang, Y.; Dostalek, J.; Knoll, W. *Anal. Chem.* **2011**, *83* (16), 6202−6207.
(53) Mahmoudpour, M.; Ezzati Nazhad Dolatabadi, J.; Torbati, M.; Pirpour Tazehkand, A.; Homayouni-Rad, A.; de la Guardia, M. *Biosens Bioelectron* **2019**, *143*, No. 111603.
(54) Dursun, A. D.; Borsa, B. A.; Bayramoglu, G.; Arica, M. Y.; Ozalp, V. C. *Talanta* **2022**, *239*, No. 123074.
(55) Kotlarek, D.; Curti, F.; Vorobii, M.; Corradini, R.; Careri, M.; Knoll, W.; Rodriguez-Emmenegger, C.; Dostálek, J. *Sens Actuators B Chem.* **2020**, *320*, No. 128380.
(56) Morgan, H.; Taylor, D. M. *Biosens Bioelectron* **1992**, *7* (6), 405−410.
(57) Pratuangdejkul, J.; Nosoongnoen, W.; Guérin, G.-A.; Loric, S.; Conti, M.; Launay, J.-M.; Manivet, P. *Chem. Phys. Lett.* **2006**, *420* (4−6), 538−544.
(58) Almonte, L.; Lopez-Elvira, E.; Baró, A. M. *ChemPhysChem* **2014**, *15* (13), 2768−2773.
(59) Gauglitz, G.; Wimmer, B.; Melzer, T.; Huhn, C. *Anal Bioanal Chem.* **2018**, *410* (3), 725−746.
(60) Jodko-Piorecka, K.; Litwinienko, G. *ACS Chem. Neurosci.* **2013**, *4* (7), 1114−1122.
(61) He, J.; Adrahtas, D. Z.; Froehlich, C. E.; Gruber, K.; Dorfman, K. D.; Frisbie, C. D.; Haynes, C. L.Small Molecule Detection with a Floating Gate Transistor Biosensor. In preparation, 2023.

https://doi.org/10.1021/acs.analchem.2c04192
Anal. Chem. 2023, 95, 2639−2644